Accepted Manuscript: https://doi.org/10.1016/j.biomaterials.2021.120966

Systemic Delivery of mRNA and DNA to the Lung using Polymer-Lipid Nanoparticles

James C. Kaczmarek [a,b,1], Asha Kumari Patel [b,c,1], Luke H. Rhym [a,b], Umberto Capasso Palmiero [b,d,#], Balkrishen Bhat [e], Michael W. Heartlein [e], Frank DeRosa [e], & Daniel G. Anderson [a,b,f,g,]*

[a] Department of Chemical Engineering, Massachusetts Institute of Technology, Cambridge, MA 02139, USA.

[b] David H. Koch Institute for Integrative Cancer Research, Massachusetts Institute of Technology, Cambridge, MA 02139, USA.

[c] National Heart & Lung Institute, Imperial College London, South Kensington, SW7 2AZ, UK.

[d] Department of Chemistry, Materials, and Chemical Engineering, Politecnico di Milano, Via Mancinelli 7, 20131, Milano, Italy.
[#] Present address: Department of Chemistry and Applied Biosciences, Institute for Chemical and Bioengineering, ETH Zurich, 8093 Zurich, Switzerland

[e] Translate Bio, Lexington, MA 02421 USA.

[f] Institute for Medical Engineering and Science, and [g] Harvard and MIT Division of Health Science and Technology, Massachusetts Institute of Technology, Cambridge, MA 02139, USA.

* Corresponding author address: Koch Institute for Integrative Cancer Research, Massachusetts Institute of Technology, 500 Main Street, Cambridge, MA 02139, USA. Email: dgander@mit.edu

[1] Equal author contribution

Abstract

Non-viral vectors offer the potential to deliver nucleic acids including mRNA and DNA into cells *in vivo*. However, designing materials that effectively deliver to target organs and then to desired compartments within the cell remains a challenge. Here, we develop polymeric materials that can be optimized for either DNA transcription in the nucleus or mRNA translation in the cytosol. We synthesized poly(beta amino ester) terpolymers (PBAEs) with modular changes to monomer chemistry to investigate influence on nucleic acid delivery. We identified two PBAEs with a single monomer change as being effective for either DNA (D-90-C12-103) or mRNA (DD-90-C12-103) delivery to lung endothelium following intravenous injection in mice. Physical properties such as particle size or charge did not account for the difference in transfection efficacy. However, endosome co-localization studies revealed that D-90-C12-103 nanoparticles resided in late endosomes to a greater extent than DD-90-C12-103. We compared luciferase expression *in vivo* and observed that, even with nucleic acid optimized vectors, peak luminescence using mRNA was two orders of magnitude greater than DNA in the lungs of mice following systemic delivery. This study indicates that different nucleic acids require tailored delivery vectors, and further support the potential of PBAEs as intracellular delivery materials.

Keywords: Gene delivery, non-viral vectors, lung, DNA, nanoparticles, mRNA

Introduction

The *in vivo* delivery of exogenous nucleic acids, such as antisense oligonucleotides,[1,2] siRNA,[3,4] DNA,[5,6] and mRNA,[7,8] has great potential to precisely treat genetic disease. In order to capitalize on this promise, however, nucleic acids must be able to reach and enter their target cells following *in vivo* administration. With few exceptions,[2,4] the delivery of large nucleic acids such as DNA and mRNA require the use of synthetic delivery vehicles that can protect their nucleic acid cargo while promoting cellular uptake and endosomal escape.[9] Although, in theory, these basic requirements of a delivery vector are the same for all nucleic acids, differences in nucleic acid size, structure, and type/degree of nucleotide modifications[4,10–13] may all play a role in the efficacy, or lack thereof, of delivery materials for specific applications. Thus, it cannot readily be assumed that a delivery vehicle that is potent for one type of nucleic acid, will be equally capable of delivering others. For example, Kauffman *et al.* optimized lipid nanoparticle formulations that were originally developed for siRNA delivery and repurposed them for mRNA delivery. They showed an 8-fold increase in mRNA potency with regards to the original formulation used for siRNA delivery, but no difference in terms of its capacity to effectively deliver siRNA *in vivo*.[14] This study, in particular, highlights two principles: 1) Adapting a nucleic acid delivery vehicle for use with a different nucleic acid may require some alterations and 2) Optimization of an existing delivery vehicle for another type of nucleic acid will not necessarily improve potency of the original payload.

Therefore, delivery of distinct nucleic acids will likely require tailored vectors. Two nucleic acids of particular interest are mRNA and DNA, where precise co-delivery may be important for applications such as CRISPR therapies that utilize guide RNA, mRNA encoding for Cas9 as well as a DNA template.[15–17] For protein replacement therapy, both mRNA and DNA can be utilized to upregulate production of a target protein; however DNA must reach the nucleus in order to effectively produce protein. The need for mitotic breakdown of the nucleus has been hypothesized as one method for DNA delivery into dividing cells[18], and is the subject of differing opinions. However, it is clear that the nucleus poses a significant barrier for DNA drugs. Recent data indicate that mRNA can lead to high peak protein levels, especially in slowly dividing or terminally differentiated cells, since it need only reach the cytoplasm in order to take effect.[19] On the other hand, plasmid DNA will typically lead to longer protein production, and has greater nuclease stability.[20] The interplay between these characteristics can be observed in a study by Zangi *et al.,* in which they show mRNA delivered by cardiac injection has a higher peak protein production, but a shorter duration of protein production, compared to DNA.[20] Progress with mRNA delivery is a relatively recent phenomenon thanks in part to improvements in the stability and function of *in vitro* transcribed mRNA.[20–25]

It has been shown that mRNA can be delivered specifically to the lung upon intravenous injection in mice using a class of materials known as poly(β-amino esters) (PBAEs).[26,27] Earlier studies had developed PBAEs, consisting of diacrylate and amine monomers, to deliver plasmid DNA (pDNA), and efficacy via intravenous administration had previously shown limited potency.[28] Subsequent studies focused on improving serum stability of the complexes either by polymer

modification[29,30], such as inclusion of a third hydrophobic alkylamine monomer to generate PBAE terpolymers[26,31], or formulation optimization such as varying the PEG-lipid ratio.[27] Here, we explore the potential of PBAE terpolymers formulated with PEG-lipid to deliver both mRNA or DNA *in vivo*. In this work, we show that PBAE nanoparticles composed of similar monomers can differ in their ability to deliver mRNA or pDNA to the lungs of mice after systemic administration. This difference is not readily correlated with any gross changes in nanoparticle characteristics, although it does correlate with differences in endosomal colocalization.

Results

Optimization of PBAE formulation and monomer chemistry for pDNA and mRNA delivery

In order to select a subset of materials for *in vivo* testing, we carried out initial experiments *in vitro* in HeLa cells. Although such rapidly dividing cells cannot fully recapitulate the barriers to pDNA delivery faced *in vivo*, we reasoned that they could be helpful for excluding ineffective particle formulations. PBAE terpolymers were synthesized as previously described,[31] using step polymerization via Michael addition between a diacrylate and two different amines; a hydrophobic amine-terminated hydrocarbon (alkylamine) and a hydrophilic amine, followed by end-capping with a diamine (Figure 1a). Nucleic acid-loaded PBAE nanoparticles were prepared via nanoprecipitation by mixing an organic phase containing polymer and 7 wt% PEG-lipid (relative to the organic phase) and an aqueous phase containing the nucleic acid in an acidic buffer (50:1 polymer to nucleic acid w/w, Figure 1b). The first study focused on lead PBAE components that were previously used to synthesize vectors for mRNA delivery,[26] based on the '**DD90**' diacrylate-amine backbone (Figure 1a). Variations of this polymer were synthesized in order to determine if synthetic parameters found to influence mRNA delivery were also important for DNA. Specifically, end-cap monomer,[28] diacrylate-amine ratio,[32] and alkylamine hydrocarbon length[31] were varied to produce a library of 30 polymers (Table S1). This library was designed in a previous study investigating mRNA delivery, using statistical methods that minimize the number of necessary experiments to scan the large synthesis space.[27] Nanoparticles were formulated using the polymers with either luciferase-encoding pDNA or mRNA and were then used to transfect HeLa cells in a 96 well plate. The cells were assayed for luminescence 24 hours after transfection (Figure 1c). As can be seen in Figure S1, there is a strong linear correlation between polymers most effective for DNA and those most effective for mRNA, with residuals regularly interspersed. We therefore opted to move forward with synthesis 'A1' which demonstrated relatively high transfection efficiency for both pDNA and mRNA namely, DD-90 incorporating a C12 alkylamine, using 1.2:1 diacrylate to amine ratio and end-capping with amine '103' (Table S1).

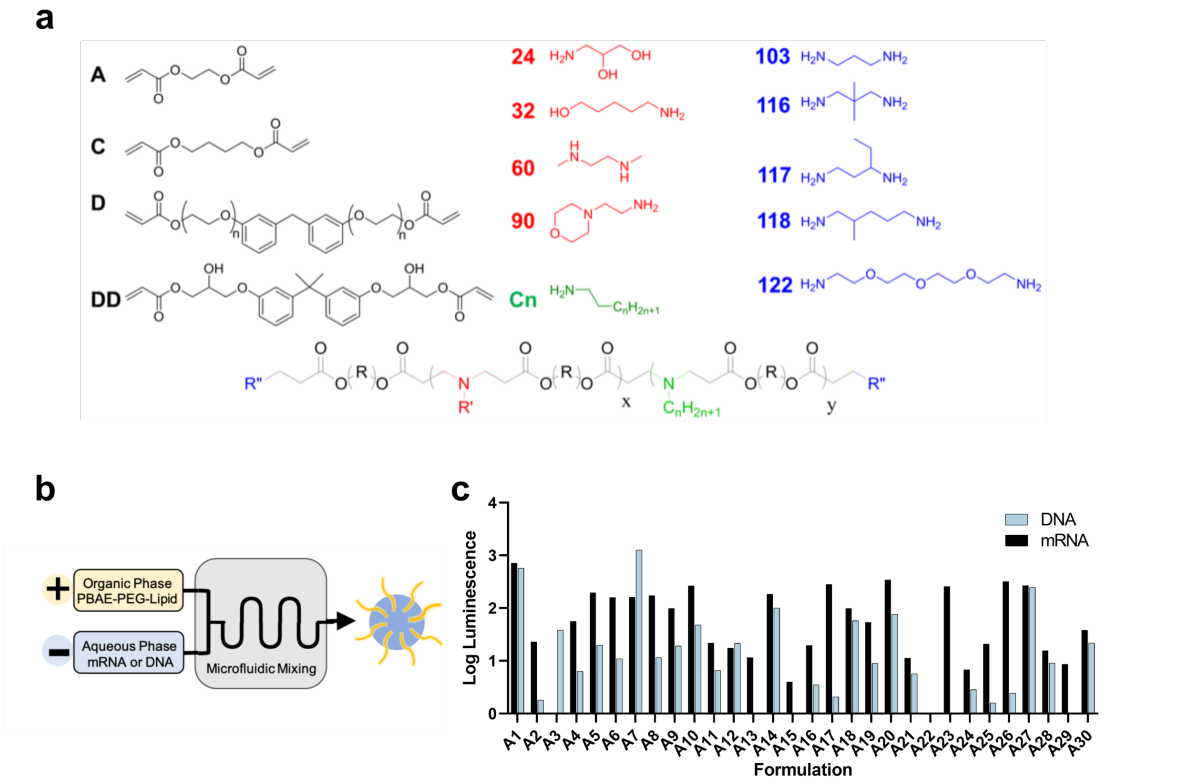

Figure 1: Synthesis of PBAEs, formulation of nanoparticles and comparison of transfection efficiency in HeLa cells. (a) A library of PBAE terpolymers were synthesized based on previous studies.[26,28,32] Terpolymers are synthesized via the Michael Addition of amines (red and green) to diacrylate monomers (black) with a molar excess of diacrylate, followed by end capping with different amines (blue). (b) Nanoparticles were formulated by microfluidic mixing of an organic phase containing PBAE and PEG-lipid with an acidic aqueous phase containing the nucleic acid, at a 1:1 v/v ratio. Electrostatic condensation yields nanoparticles which are PEGylated as a result of hydrophobic interactions between the alkylamine side chains and the hydrocarbon tail of the PEG-lipid. (c) A library of 30 PBAEs based on DD-90 with different alkylamines, end cap amines, and PEG-lipid ratio were formulated with either DNA or mRNA encoding firefly luciferase and delivered to HeLa cells in a 96 well plate (n=4), formulation parameters are detailed in table S1.

Next, we wanted to directly compare the ability of PBAEs synthesized using various backbone acrylate and amine monomer combinations to deliver pDNA or mRNA in HeLa cells. Sixteen polymers were prepared using all combinations of the diacrylate and non-alkylated amines shown in Figure 1a, keeping the 'C12' alkylamine and '103' end cap amine consistent as determined by our first study. Using the same transfection procedure as was just described, we observed that, in general, the best polymers for mRNA delivery were also the most effective for DNA delivery (Figure 2a). Additionally, both mRNA and DNA produced similar levels of luminescence at the 24 hour time point despite likely differences in optimization performed in synthesizing the pDNA (obtained commercially from Aldevron) and the mRNA (supplied by Translate Bio). The **DD90-C12-103** polymer which was previously identified as optimal for mRNA delivery was also the most

effective for DNA *in vitro* (Figure 2a). However, because HeLa cells rapidly divide, and thus experience multiple periods of nuclear permeability, the additional hurdle of nuclear localization cannot be accurately assessed using this cell line. Consequently, we transfected primary mouse lung endothelial cells with DD90-C12-103 formulated with mRNA or pDNA encoding for luciferase (Figure 2b). In primary cells, pDNA transfection with DD90-C12-103 particles was relatively low compared to mRNA.

Due to the differences observed between cell line and primary cell transfection efficiency, we moved multiple candidates forward for *in vivo* testing. Since early studies with PBAE terpolymers injected systemically revealed that amines **32** and **90** typically resulted in serum stable nanoparticles, while amines **60** and **24** did not,[26] we decided to move forward with the top performing nanoparticles from each group of PBAEs which shared a diacrylate. Thus, **A32-C12-103**, **C32-C12-103**, **D90-C12-103**, and **DD90-C12-103** were selected for *in vivo* studies. As this subset of PBAEs share the same alkylamine 'C12' and end cap amine '103', herein we will annotate each PBAE with only the diacrylate and non-alkylated amine ie. **A32**, **C32**, **D90** and **DD90**.

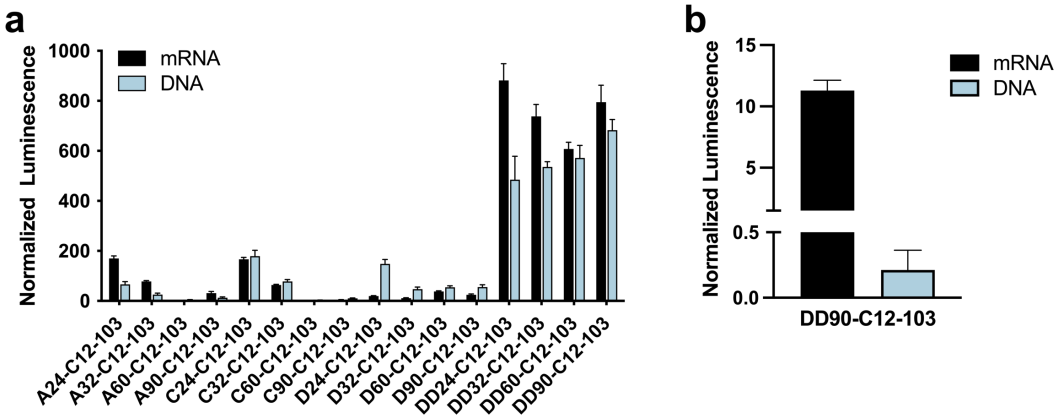

Figure 2: PBAE transfection of HeLa and primary mouse lung endothelial cells with mRNA and DNA. (a) Chemically diverse PBAE terpolymer nanoparticles were formulated using optimal parameters screened in figure 1 and used to transfect HeLa cells in a 96 well plate with either luciferase encoding mRNA or DNA. A wide range of bioluminescence was observed. DD90-C12-103 demonstrated relatively high efficacy for both DNA and mRNA transfection in HeLa cells. (b) Primary lung endothelial cells from mice were transfected with DD90-C12-103 particles containing either mRNA or DNA encoding luciferase. (n=4, all experiments).

In vivo Screen for DNA Efficacy and Biodistribution

Having chosen a subset of PBAEs for *in vivo* testing, we proceeded to formulate particles containing luciferase-encoding DNA plasmids for intravenous injection in mice. PEGylated particles were formulated as described earlier for *in vitro* testing using nanoprecipitation (Figure 1b) and injected via the tail vein into mice at a dose of 0.5 mg/kg (nucleic acid/mouse weight). In addition, a commercially available transfection reagent in vivo-JetPEI, and the 'C12-200' vector

originally developed for siRNA delivery but also capable of mRNA delivery[14], were also tested for DNA delivery. Mice were sacrificed 24 hours post-injection and their organs harvested for luminescent imaging. The **C32** formulation resulted in immediate mortality in mice, these formulations were visibly turbid presumably due to serum instability.[26,33] Of the 3 remaining PBAEs, **D90** complexes achieved the highest DNA mediated luminescence in the lung (9.88 x 10^5 RLU), approximately 2 orders of magnitude greater than **DD90** (8.09 x 10^3 RLU), **A32** (1.90 x 10^4 RLU), JetPEI (6.24 x 10^3) and C12-200 (3.90 x 10^2) (Figure 3).

Interestingly, when **DD90** was optimized for systemic delivery of mRNA in a previous study, highly efficient translation was observed primarily in the lung[27]. However, in this study we found that **DD90** had similar levels of DNA transfection in the lung, liver and spleen potentially due to differences in synthetic parameters outlined earlier (Table S1). In contrast, DNA delivery using the **D90** vector was mainly observed in the lung (Figure 3). To assess which lung cell sub-types were being transfected with **D90**, we delivered pDNA encoding for Cre-recombinase to Ai14 reporter mice. Flow cytometry of lung tissue found that 20.6 % (± 4.2) of the endothelial cell population was transfected and 1.2 % (± 0.3) immune cells were transfected (figure S2a).

Due to the efficient mRNA delivery to the lung observed in our previous study using **DD90** vectors[27] and the superior DNA delivery seen in this study using **D90** vectors, these two PBAEs were taken forward for comparison studies between mRNA and DNA delivery *in vivo*.

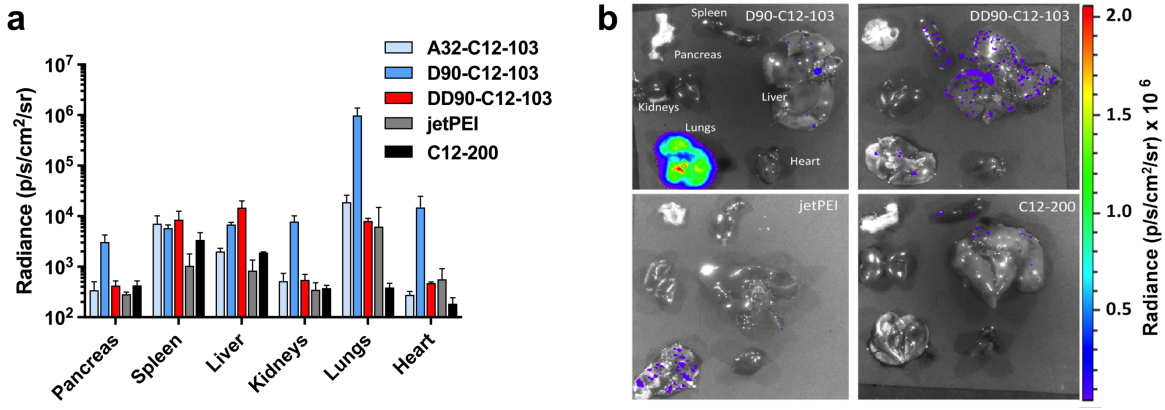

Figure 3: *In vivo* screen for DNA efficacy. Mice were injected with various PBAEs formulated with luciferase-encoding DNA at a dose of 0.5 mg/kg. (a) 24 hours following injection, organ luminescence was quantified via IVIS. In most organs, most notably the lungs, **D90-C12-103** surpasses other transfection reagents in terms of DNA efficacy by 1-2 orders of magnitude. (b) Luminescent images showing the biodistribution of luciferase expression following treatment with various nanoparticles (*n*=3).

In vivo comparison of protein expression mediated by mRNA versus DNA

Next, we wanted to compare the relative amount of protein produced *in vivo* following delivery of mRNA or DNA using the selected **D90** and **DD90** PBAEs. In addition, we were also interested in observing the kinetics of protein production over time using DNA compared to mRNA. We intravenously injected PBAE nanoparticles loaded with luciferase-encoding mRNA or pDNA into hairless, immunocompetent mice at a dose of 0.25 mg/kg of nucleic acid. Luminescent images of whole mice were taken at various time points and quantified (Figure 4). Overall, mRNA delivery was optimal using **DD90-mRNA** complexes compared to **D90-mRNA** and conversely, DNA delivery was superior using **D90-DNA** (Figure. 4). In terms of peak protein expression, as before, DNA resulted in less protein production than mRNA which generated over 2 orders of magnitude higher luminescence (1.18 x 10^9 p/s) at 24 hours, compared to DNA (4.4 x 10^6 p/s) (Figure 4 a,b). Previous studies have shown that protein production mediated by DNA lasts longer, albeit with a lower peak,[20] which one might expect given the superior nucleic acid stability, therefore we also calculated area under the curve (Figure 4c). Surprisingly, the kinetics of protein expression following DNA delivery were almost identical to those resulting from mRNA delivery and resulted in lower total bioluminescence by almost 2 orders of magnitude compared to mRNA (Figure 4c). This may be attributed to episomal transgene silencing, a commonly observed phenomena previously described following plasmid DNA delivery *in vivo* using certain promoters.[34]

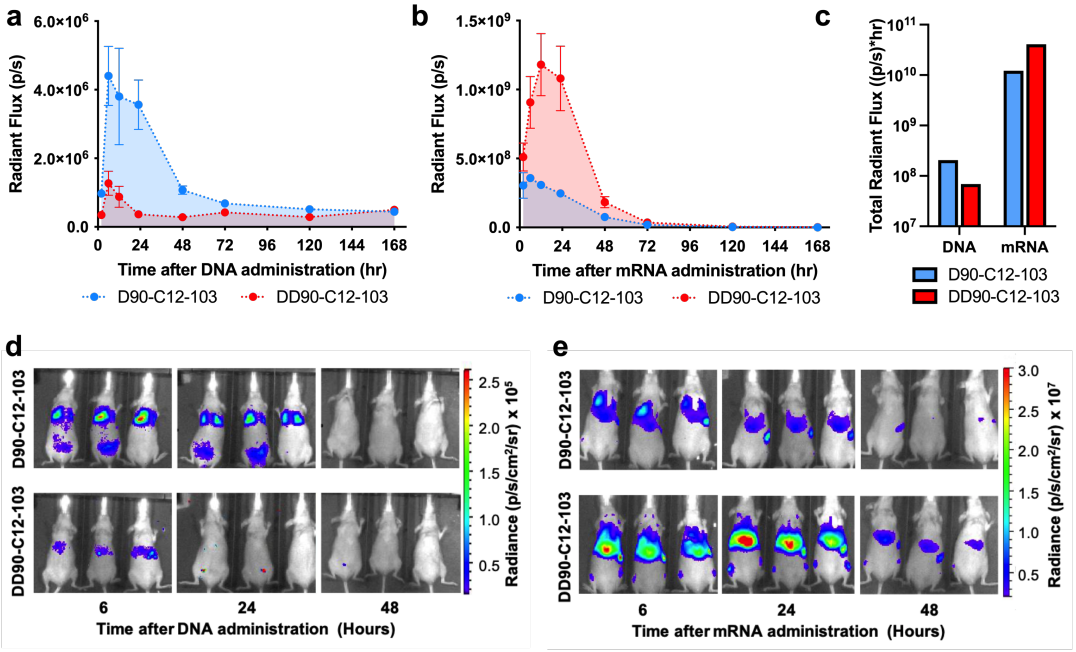

Figure 4: Time course expression studies *in vivo*. Hairless, immunocompetent mice received tail-vein injections of either DNA (a, d) or mRNA (b, e) encoding for luciferase at a dose of 0.25 mg/kg. Live mice were imaged at various time points following the injection. (c) Area under the curve analysis shows that absolute bioluminescence is greater with mRNA compared to DNA with both vectors, note difference in Y scale for charts (a) and (b). . Surprisingly, DNA expression follows roughly the same kinetics as mRNA expression.

Nanoparticle Characterization

To examine the relationship between particle properties and function, we measured nanoparticle size, zeta potential, and DNA encapsulation efficiency of **D90** and **DD90** vectors. Of these parameters, both zeta potential[35] and encapsulation efficiency[36] have been correlated, to some degree, with nanoparticle delivery efficacy, and in our previous work we demonstrated that size correlates with biodistribution of luciferase mRNA translation using systemically delivered PBAE nanoparticles.[27] We were also interested in observing the size and zeta potential of particles over a range of pH, due to the acidification that is experienced within the endosome.[37] As can be seen in Figure 5, both zeta potential (over the full range of pH tested) and DNA encapsulation efficiency of **D90** and **DD90** were very similar. The only significantly different measured property between **D90** and **DD90** DNA nanoparticles was size (Figure 5b), at all pH levels tested **DD90** particles were both larger and more variable in size between batches than those composed of D90 when formulated at 7 % PEG-lipid. For example, at physiological pH, **DD90-DNA** complexes were 326 nm (± 68) whereas **D90-DNA** nanoparticles were 162 nm (±3.4) (Figure 5b). To investigate whether smaller particle size could improve DNA delivery using **DD90**, we increased the PEG-lipid content to 15 %, which was previously found to improve systemic mRNA delivery to the lung.[27] This reduced **DD90-DNA** particle diameter to 204 nm however, this did not result in luciferase expression that rivaled that of **D90-DNA** following systemic injection (Figure S3b).

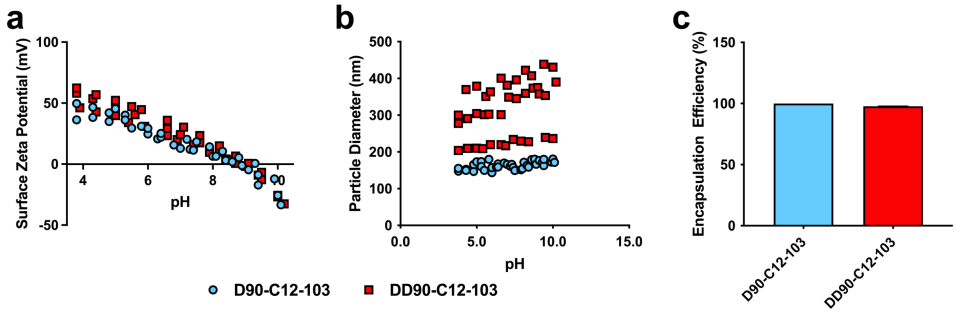

Figure 5: Nanoparticle physical characterization. Nanoparticle size (a) and zeta potential (b) were measured over a range of pH values for DNA-loaded **D90-C12-103** and **DD90-C12-103**. Nanoparticle encapsulation efficiency (c) was measured in TE buffer near physiological pH. The only gross difference in nanoparticle physical characteristics was size, although size alone did not appear to correlate with increased efficacy of DNA delivery (Figure S3). Size and zeta potential measurements reported as aggregates of 3 separate batches of nanoparticles, while encapsulation efficiency data was reported as an average (n=3).

Endosomal Trafficking of DNA delivered using D90 or DD90 nanoparticles

In light of the limited correlation between gross nanoparticle properties and increased ability to deliver DNA, we examined endosomal trafficking of **D90** and **DD90** DNA nanoparticles formulated with 7 % PEG-lipid. Trafficking between early and late endosomes has been correlated previously with both siRNA[38] and mRNA[39] delivery efficacy, but mainly in the context of lipid nanoparticles. To evaluate the endosomal localization of our PBAE nanoparticles, we formulated **D90** and **DD90**

particles as before with fluorescently-labeled DNA plasmid. We carried out the study in HeLa cells and in primary mouse lung endothelial cells. After a 3 hour incubation with the nanoparticles containing the fluorescently-labeled plasmid, media was replaced and cells were subjected to a further 15, 30, or 60 minute incubation, at which points they were fixed and stained. Co-localization analysis with markers for early endosomes (EEA1) and late endosomes (LAMP1) revealed that both **D90** and **DD90** nanoparticles rapidly localized to late endosomes (Figure 6). **D90** however, localized with late endosomes to a significantly greater extent than **DD90** at 15 mins in both HeLa and primary lung endothelial cells**.** Late endosome co-localization of **D90** was greater than **DD90** at all timepoints in HeLa cells, however in primary mouse lung endothelial cells, **DD90** co-localization with late endosomes increases to a level comparable to **D90** at 30 and 60 mins. Such mature, late endosomes are typically located closer to the nucleus than early endosomes,[37] which suggests that such localization may play a role in delivery. However, this trend seems to be less apparent in primary cells compared to rapidly dividing HeLa cells.

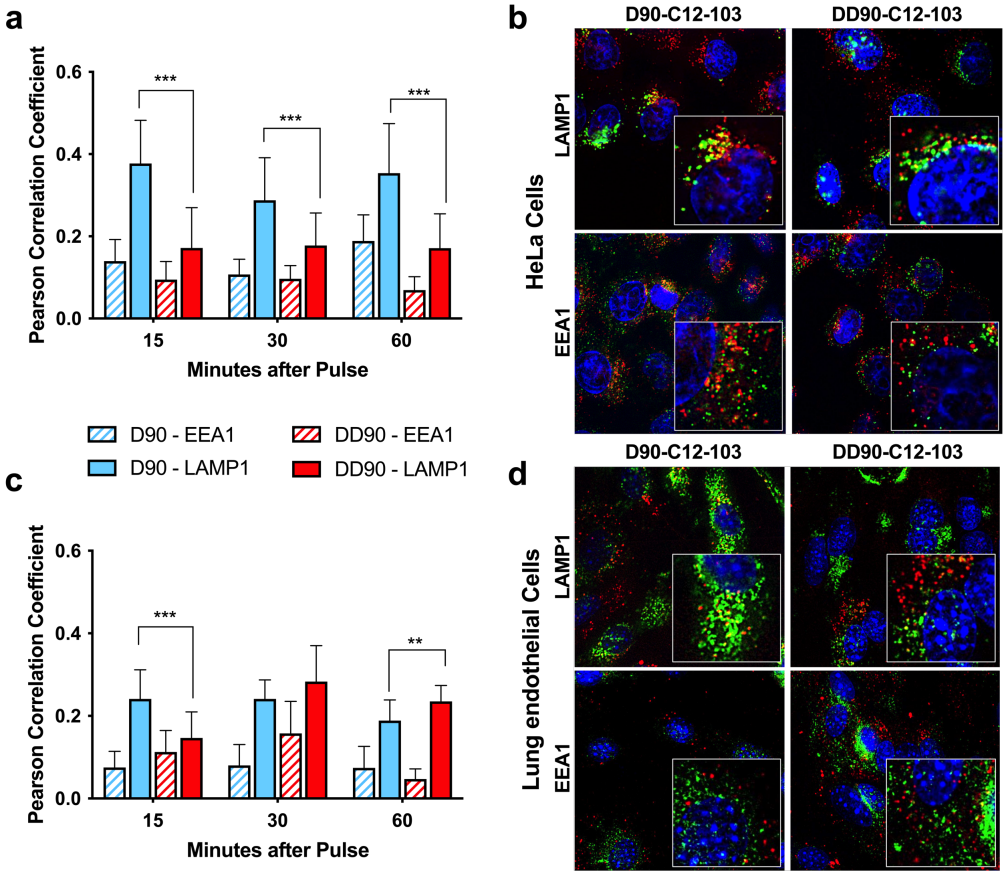

Figure 6: Nanoparticle endosomal trafficking studies of pDNA in primary mouse lung endothelial cells and HeLa cells. D90-C12-103 and DD90-C12-103 nanoparticles were loaded with Cy5-labeled pDNA (red) and used to transfect HeLa cells at a dose of 0.5 ng/uL (a-b) or primary mouse lung endothelial cells at a dose of 1.5 ng/uL (c-d). Three hours following transfection, nanoparticles were washed and incubated with fresh media for 15, 30, or 60 minutes, at which point they were fixed and stained for markers of early (EEA1, green) or late endosomes (LAMP1, green) and the nucleus (DAPI, blue). (a, c) Quantification of Cy-5 and endosomal marker colocalization using ImageJ (n > 20 cells). (b, d) Representative images of the various transfection/staining conditions at 60 minutes (b) or 15 minutes (d). *** $p<0.001$, ** $p<0.01$.

Discussion

Recent advances in the *in vitro* transcription and delivery of mRNA have led to its reemergence as an alternative to plasmid DNA for protein replacement therapy using nucleic acids.[7,19] Although more prone to degradation than DNA, mRNA need only reach the cytoplasm to yield protein production, eliminating the hurdle of crossing the nuclear membrane. However, outside of some direct injection[20] and *in vitro* studies,[40] less direct comparison of exogenous plasmid DNA and mRNA delivery *in vivo* has been described.[41,42]

Our initial studies using a library of 30 PBAEs (Table S1) in HeLa cells demonstrated correlation between materials that were effective for mRNA delivery and those that were effective for DNA delivery using luciferase as a reporter gene (Figure 2a). We synthesized a further library of 16 polymers, which varied the diacrylate-amine backbone but kept the alkylamine 'C12' and end cap amine '103' consistent. From this subset, **DD90-C12-103** nanoparticles, which had previously been identified as capable of delivering mRNA,[26,27,43] were also the most effective for pDNA delivery *in vitro* (Figure 2b). Moreover, there was little difference between the two nucleic acids in terms of luminescence at the 24-hour time point across all 16 materials tested (Figure 2b), suggesting similar inherent capacity of these particular constructs to produce luciferase protein in HeLa cells. The *in vivo* results, however, demonstrated that DNA, in general, was much less capable of inducing protein production than mRNA by two orders of magnitude (Figure 4), with **D90-C12-103** being the most efficient DNA delivery vector when administered by tail vein injection (Figure 3) and **DD90-C12-103** remaining most effective for mRNA delivery (Figure 4).

The large relative difference in *in vitro* and *in vivo* efficacy between DNA and mRNA, may be due to differences in the additional hurdle of crossing the nuclear membrane in slower dividing cells, or transcript differences such as codon optimization, promoters and UTR sequences that influence transcription or translation efficiency.[19] For example, it has been hypothesized that rapid division of cell lines, such as HeLa result in periods of time in which the nuclear membrane is permeable to the cytosol, making it easier for DNA to cross the nuclear membrane *in vitro* than in most cells *in vivo*[18]. While it is possible that the overall process of transcription is less efficient *in vivo* than in HeLa cells, it has been observed that protein abundance is generally controlled on a translational level. Overall expression of protein from mRNA is affected by the 5' and 3' UTRs, polyA tail, cap, and codons. For DNA, first the promoter leads to differing amounts of mRNA, followed by mRNA processing and export to the cytoplasm, and then all of the mRNA structural issues apply.[44] When thymidine is used to arrest cellular division, a reduction in potency is observed for both mRNA and DNA (Figure S4) possibly due to a reduction in general protein synthesis as a result of S-phase cell synchronization (Figure S5).[45] Nonetheless, it is evident that in non-dividing cells, there is a greater reduction in DNA-mediated luciferase expression compared to mRNA (Figure S4). It may be that other differences between *in vitro* and *in vivo* translation, such as endocytosis by target cell populations,[46] endosomal escape,[47] and particle stability in serum,[28] also affect the observed potency disparity between mRNA and DNA.

Despite the substantially reduced protein expression by formulations delivering DNA compared to mRNA, we have observed that **D90-C12-103** was more effective than other materials for DNA

delivery *in vivo*, and not mRNA delivery. One hypothesis is that certain nanoparticles may facilitate crossing the nuclear membrane. Indeed, Figure 3 shows that all PBAEs tested were at least somewhat more capable of DNA delivery than the lipid nanoparticle formulated with C12-200, despite C12-200's superior capacity for mRNA delivery.[27] We also noted that **D90-C12-103** nanoparticles had an increased colocalization with late endosomes compared to **DD90-C12-103** in HeLa cells and at early timepoints in primary mouse lung endothelial cells (Figure 6). It is possible that endosomal trafficking to the perinuclear region may play a role in pDNA delivery to the nucleus. However, we note that C12-200 lipid formulations for siRNA delivery to the cytosol have previously been shown to have high colocalization with late endosomes compared to early endosomes yet we observed a relative inability of C12-200 to deliver DNA (Figure 3b).[38] Moreover, we note that in the primary cells, **DD90-C12-103** eventually co-localized with late endosomes to a similar degree. We were not able to further correlate such trafficking, or overall plasmid DNA efficacy, with physical properties of the nanoparticles (Figure 5). DD90-C12-103 particles were larger when formulated with DNA compared to D90-C12-118 which may influence biodistribution of particles. Smaller particles were therefore formulated by increasing the percentage of PEG-lipid to 15 %, however this did not achieve greater DNA transfection (Figure S2), even though this strategy has previously improved mRNA transfection of the lung.[27] More advanced characterization methods, for example those that can examine the structure of the nanoparticle in greater detail,[48] maybe helpful to further investigate differences between **D90-C12-103** nanoparticles and those formulated using other polymers that may lead to enhanced nuclear localization.

Previous studies have reported that pDNA results in more sustained protein expression compared to mRNA[20]. Figure 4 demonstrates that in these experiments the kinetics of protein expression following mRNA and DNA delivery are roughly similar. Other studies have shown that bacterial elements within the DNA backbone can induce promoter inactivation, which ultimately results in silencing of the transgene.[34,49] However, most of these studies show a slow decline in DNA expression over the period of days,[50–52] whereas we observe rapid decay of plasmid expression over a period of hours. It is possible that these PBAE/DNA vectors act to stimulate an immune response that is shutting off the promoters.[53] Such a phenomena may also explain why a systemic injection of nanoparticles would behave differently in terms of expression kinetics than local administration.[20] It is also possible that the plasmid promoter of this particular DNA construct may be unstable, as previous studies have reported that the length of DNA expression is strongly dependent on promoter.[54] Thus, it is likely that a different promoter and/or the removal of bacterial elements from the plasmid backbone, such as minicircle DNA,[34] would result in sustained transgene expression in the context of PBAE-mediated delivery.

In conclusion, we have identified significant differences in mRNA and DNA delivery by PBAEs *in vivo* by making only slight modifications to one monomer in the polymer backbone. Although *in vivo* delivery of DNA was substantially less efficient in terms peak protein production, and no more efficient in terms of duration of protein production than mRNA, all PBAEs tested were at least moderately more capable of plasmid DNA delivery than the lipid C12-200 and JetPEI. Our screen identified **D90-C12-103** as the most effective vector for delivery of DNA. Our findings provide

mechanistic insight into this difference through correlating **D90-C12-103**'s increased DNA potency with an increase in late endosomal localization compared to **DD90-C12-103**. Differences in nanoparticle physical properties such as size was observed but size alone could not be correlated to increased transfection capability. These materials provide a basis for further mechanistic evaluation into the delivery of different nucleic acids, which could ultimately help enable the rational design of delivery vehicles tailored to specific intracellular targets.

Materials and Methods

Materials

Bisphenol A glycerolate diacrylate (DD), bisphenol A ethoxylate (M_n~468, 1.5 EO/phenol) diacrylate (D), ethylene glycol diacrylate (A), 4-(2-amino methyl) morpholine (90), N-N'-dimethyl ethylene diamine (60), (+/-)-3-amino-1,2-propanediol (24), dodecyl amine (C12), octyl amine (alkylamine C8), octadecyl amine (alkylamine C18), 1,3-diaminopropane (end cap 103), 1,3-diaminopentane (end cap 117), 2-methyl-1,5-diaminopentane (end cap 118), and cholesterol were purchased from Aldrich (St. Louis, MO). (Poly-ethylene oxide)$_4$-bis-amine (122) was purchased from Molecular Biosciences (Boulder, CO, USA). 1,4-butanediol diacrylate (C), 5-amino-1-pentanol (32), and heparin sodium salt from porcine intestinal mucosa were obtained from Alfa Aesar (Haverhill, MA, USA). 14:0 PEG2000 PE (PEG-lipid) and 1,2-dioleoyl-sn-glycero-3-phosphoethanolamine (DOPE) were purchased from Avanti Polar Lipids (Alabaster, AL, USA). C12-200 was purchased from WuXi AppTech (Shanghai, China). I*n vivo* jetPEI (Polyplus) was obtained from VWR (Radnor, PA). gWiz luciferase-encoding DNA plasmid was purchased from Aldevron (Fargo, ND). Firefly luciferase-encoding mRNA was generously provided by Translate Bio (Lexington, MA, USA). All chemical reagents were used as received with no further purification.

Polymer Synthesis

All monomers were pre-dissolved in anhydrous dimethylsulfoxide at a concentration of 1 M. The appropriate amount of diacrylate, primary amine, and alkylamine were mixed together and reacted at 90°C for 48 hours. Following this reaction, an excess of end-capping amine was added and reacted at room temperature for an additional 24 hours. Polymers were then further diluted in DMSO to a concentration of 100 mg/mL of non-end capping monomer and were stored at -80°C until needed. In a typical synthesis of DD90-C12-103, to a 5 mL glass scintillation vial were added the bisphenol A glycerolate diacrylate (200 mg, 0.41 mmol, 1.2 equiv), 4-(2-amino methyl) morpholine (22 mg, 0.17 mmol, 0.5 equiv), and dodecyl amine (32 mg, 0.17 mmol, 0.5 equiv). The vial was then sealed, covered in aluminum foil, and heated to 90ºC. After 48 hours, the reaction was cooled to room temperature. The vial was opened to the air and end-capping amine 1,3-diaminopropane was added in excess (38 mg, 0.51 mmol) and mixed until completely dissolved. The end-capping reaction was allowed to proceed at room temperature for 24 hours, followed by dilution in DMSO. A general reaction scheme can be found in the supporting information.

mRNA and DNA

Luciferase-encoding mRNA was a generous gift from Translate Bio, and was synthesized by an *in vitro* transcription from a plasmid DNA template encoding for the firefly luciferase gene. The *in vitro* transcription was followed by the addition of a 5' cap structure (Cap1) using a vaccinia virus-based guanylyl transferase system. FLuc mRNA contained a 5' UTR consisting of a partial sequence of the cytomegalovirus (CMV) immediate early 1 (IE1) gene, a coding region as described below, a 3' UTR consisting of a partial sequence of the human growth hormone (hGH) gene, and a 3' polyA tail (~300 nt).

AUGGAAGAUGCCAAAAACAUUAAGAAGGGCCCAGCGCCAUUCUACCCACUCGAAGACGG
GACCGCCGGCGAGCAGCUGCACAAAGCCAUGAAGCGCUACGCCCUGGUGCCCGGCACC
AUCGCCUUUACCGACGCACAUAUCGAGGUGGACAUUACCUACGCCGAGUACUUCGAGAU
GAGCGUUCGGCUGGCAGAAGCUAUGAAGCGCUAUGGGCUGAAUACAAACCAUCGGAUC
GUGGUGUGCAGCGAGAAUAGCUUGCAGUUCUUCAUGCCCGUGUUGGGUGCCCUGUUCA
UCGGUGUGGCUGUGGCCCCAGCUAACGACAUCUACAACGAGCGCGAGCUGCUGAACAG
CAUGGGCAUCAGCCAGCCCACCGUCGUAUUCGUGAGCAAGAAAGGGCUGCAAAAGAUC
CUCAACGUGCAAAAGAAGCUACCGAUCAUACAAAAGAUCAUCAUCAUGGAUAGCAAGACC
GACUACCAGGGCUUCCAAAGCAUGUACACCUUCGUGACUUCCCAUUUGCCACCCGGCU
UCAACGAGUACGACUUCGUGCCCGAGAGCUUCGACCGGGACAAAACCAUCGCCCUGAU
CAUGAACAGUAGUGGCAGUACCGGAUUGCCCAAGGGCGUAGCCCUACCGCACCGCACC
GCUUGUGUCCGAUUCAGUCAUGCCCGCGACCCCAUCUUCGGCAACCAGAUCAUCCCCG
ACACCGCUAUCCUCAGCGUGGUGCCAUUUCACCACGGCUUCGGCAUGUUCACCACGCU
GGGCUACUUGAUCUGCGGCUUUCGGGUCGUGCUCAUGUACCGCUUCGAGGAGGAGCU
AUUCUUGCGCAGCUUGCAAGACUAUAAGAUUCAAUCUGCCCUGCUGGUGCCCACACUAU
UUAGCUUCUUCGCUAAGAGCACUCUCAUCGACAAGUACGACCUAAGCAACUUGCACGAG
AUCGCCAGCGGCGGGGCGCCGCUCAGCAAGGAGGUAGGUGAGGCCGUGGCCAAACGC
UUCCACCUACCAGGCAUCCGCCAGGGCUACGGCCUGACAGAAACAACCAGCGCCAUUCU
GAUCACCCCCGAAGGGGACGACAAGCCUGGCGCAGUAGGCAAGGUGGUGCCCUUCUUC
GAGGCUAAGGUGGUGGACUUGGACACCGGUAAGACACUGGGUGUGAACCAGCGCGGCG
AGCUGUGCGUCCGUGGCCCCAUGAUCAUGAGCGGCUACGUUAACAACCCCGAGGCUAC
AAACGCUCUCAUCGACAAGGACGGCUGGCUGCACAGCGGCGACAUCGCCUACUGGGAC
GAGGACGAGCACUUCUUCAUCGUGGACCGGCUGAAGAGCCUGAUCAAAUACAAGGGCU
ACCAGGUAGCCCCAGCCGAACUGGAGAGCAUCCUGCUGCAACACCCCAACAUCUUCGAC
GCCGGGGUCGCCGGCCUGCCCGACGACGAUGCCGGCGAGCUGCCCGCCGCAGUCGUC
GUGCUGGAACACGGUAAAACCAUGACCGAGAAGGAGAUCGUGGACUAUGUGGCCAGCC
AGGUUACAACCGCCAAGAAGCUGCGCGGUGGUGUUGUGUUCGUGGACGAGGUGCCUAA
AGGACUGACCGGCAAGUUGGACGCCCGCAAGAUCCGCGAGAUUCUCAUUAAGGCCAAG
AAGGGCGGCAAGAUCGCCGUGUAA

Luciferase-encoding DNA (gWiz Luc) was purchased from Aldevron (Fargo, ND). Construct details and sequence can be found on Aldevron's website.

Nanoparticle Synthesis

mRNA was diluted in 25 mM sodium acetate (NaOAc) buffer, pH 5.2, while the appropriate amounts of polymer and PEG-lipid (C14-PEG2000) were co-dissolved in 200 proof ethanol. For all PBAE nanoparticles, the weight ratio of polymer to nucleic acid was 50:1 and the weight percentage of PEG-lipid in the organic phase was 7 wt% with respect to PEG-lipid and polymer content. The two phases were mixed at a 1:1 v/v ratio in a microfluidic device[55] to form nanoparticles. Nanoparticles were then dialyzed against PBS (for transfection experiments) or deionized water (for characterization experiments) in a 20000 MWCO cassette at 4°C for 2-3 hours. C12-200 nanoparticles were formulated in a similar fashion, using a 3:1 ethanol to aqueous

v/v ratio. The ethanol phase was comprised of C12-200, cholesterol, DOPE, and PEG-lipid as previously described.[14] jetPEI nanoparticles were made according to supplier protocol. Briefly, jetPEI and RNA were diluted in equal volumes of the provided buffer in order to yield the desired N/P. The jetPEI phase was added to the RNA phase and was mixed by vortexing, and the resulting nanoparticles were incubated at room temperature for 15 minutes prior to use. All particles were used no earlier than 15 minutes and no later than 4 hours following synthesis/dialysis. Doses reported are in terms of total nucleic acid content in nanoparticle suspension.

Nanoparticle Characterization

For pH-dependent size and zeta potential measurements, nanoparticles were diluted to a final concentration of 5 ng/μL in 10 mL of water. Nanoparticle size was measured via dynamic light scattering using a Nano ZS (Malvern, UK), with the pH titrations performed by an MPT-2 titrator (Malvern, UK) attached the system. Surface zeta potential as reported is the average surface zeta potential, and the reported size is the peak of the intensity curve. The average of 2 technical replicates is reported for each point in the size/zeta potential vs. pH measurements. Any size measurements that did not utilize the titration were done in PBS and also used a Nano ZS apparatus. For encapsulation efficiency, a modified Quant-iT RiboGreen (Thermo Fisher, MA) assay was used. A nanoparticle dilution of ~1 ng μL^{-1} DNA was made in TE buffer (pH 8.5) and DNA standards were made ranging from 2 ng μL^{-1} to 0.125 ng μL^{-1}. 50 μL of each solution was added to separate wells in a 96-well black polystyrene plate. To each well was added either 50 μL of 10 mg/mL heparin in TE buffer, which disrupted the electrostatic forces binding the polymer and mRNA to allow for accurate quantification of nanoparticle DNA content, or 50 μL of un-supplemented TE buffer. The plate was incubated at 37ºC for 1 hour with shaking at 350 rpm. Following the incubation, the diluted RiboGreen reagent was added (100 μL per well), and the plate was incubated as before for 3 minutes. RiboGreen fluorescence was measured according to the supplied protocol using a Tecan plate reader, and the DNA standard was used to determine nanoparticle DNA concentration. It should be noted that two separate standards were made: one with and one without 10 mg/mL heparin. The particles in heparin were used to determine DNA concentration, and encapsulation efficiency was determined via the following equation, where $Conc_{TE}$ and $Conc_{Hep}$ are the concentration readings for particles without and with heparin, respectively:

$$EE = \left(1 - \frac{Conc_{TE}}{Conc_{Hep}}\right)$$

Other particle concentrations were calculated by measuring volume change before and after dialysis.

In vitro *Transfections*

All cells were incubated in a controlled environment at 37°C and 5% CO_2. HeLa cells (ATCC, VA) were cultured in Dulbecco's Modified Eagle Medium (Invitrogen, CA) supplemented with 10% v/v heat inactivated fetal bovine serum (Invitrogen, CA) and 1% v/v Penicillin Streptomycin (Invitrogen, CA). For luciferase mRNA/DNA transfections, 24 hours before transfection, cells were seeded onto a 96-well polystyrene tissue culture plate (15-20,000 cells per well, 100 μL media containing serum and antibiotic per well). In a typical example, mRNA/DNA-loaded nanoparticles were diluted to 2 ng/μL in buffer and mixed with media such that the volume ratio of nanoparticle solution to media was 1:9 (final concentration of nanoparticles 0.2 ng/µL). The media in the plate was aspirated, and the nanoparticle-containing media was added to the wells, in this case at a final concentration of 20 ng nucleic acid per well. 24 hours following transfection, cell viability was assayed using a MultiTox-Fluor Multiplex Cytotoxicity Assay (Promega, WI) or PrestoBlue assay (Thermo Fisher, MA) and cellular luminescence was quantified using Bright-Glo Assay kits (Promega, WI), both of which were measured using a Tecan plate reader. Cellular luminescence was normalized to live cell fluorescent signal. No wash step was used following particle transfection.

C57BL/6 mouse primary mouse lung microvascular endothelial cells (CellBiologics, IL) were cultured in complete endothelial cell medium (CellBiologics, IL). 2-7 days prior to transfection, cells were plated on a 24 well plate (500 μL per well). Nanoparticles were formulated and administered to cells as described for HeLa cells, with a typical final concentration of 0.5-2 ng/µL. Three hours following transfection, nanoparticle-containing media was aspirated from the wells and replaced with fresh media. Cellular viability and luminescence was assessed 24 hours after transfection as in the case of HeLa cells. All cell culture plates and flasks were pre-treated with gelatin coating solution (CellBiologics, IL).

For HeLa cells subjected to a thymidine block, cells were seeded in a 96 well plate 48 hours before transfection (7500 cells/well, 100 μL media containing serum and antibiotic per well). 24 hours prior to transfection, cells were treated with 2 mM thymidine (Aldrich, MO) to arrest cell division in S phase. For transfection, nanoparticles were prepared and diluted as described above, except the dilution was done in media containing 2 mM thymidine. Cells were assayed for luminescence as described above 24 hours following transfection.

For endosomal trafficking experiments, HeLa cells or primary mouse lung endothelial cells were seeded into glass-bottomed chamber well slides 24 hours (HeLa) or 1 week (primary cells) before transfection. Nanoparticles were formulated with Cy5-labeled DNA, which was produced by labeling the Aldevron gWiz plasmid using the Cy5 Label IT reagent (Mirus, WI) as directed. The nanoparticles were diluted in PBS at a volume of 5 ng/µL (HeLa) or 15 ng/µL (primary cells), which was then diluted in cell culture media at a 1:9 v/v ratio. The media in the slide chambers was then aspirated and the nanoparticle containing media was added. Three hours following the transfection, the nanoparticle-containing media was aspirated and cells were washed 1-3x with PBS. Fresh media was then added to the nanoparticles. At 15, 30, or 60 minutes following the wash, cells were washed 3x with PBS and fixed in 4% paraformaldehyde for 10-15 minutes. Cells were then washed an additional 3x with PBS and were then incubated in permeabilization buffer (4% normal goat serum, 1% bovine serum albumin, and 0.05% Tween 20 in PBS) for 1 hr. at room temperature. Cells were then treated with primary antibodies diluted in permeabilization buffer overnight at 4°C. Antibodies for HeLa cells were mouse anti-EEA1, BD clone 14/EEA1 (5 µg/mL) and mouse anti-LAMP1, Abcam clone H4A3 (5 µg/mL). Antibodies for primary cells were

rabbit anti-EEA1, abcam ab2900 (1 µg/mL) and rabbit anti-LAMP1, abcam ab24170 (5 µg/mL). Following primary incubation, cells were washed 5-6x over the course of 1 hr. using PBS and were then incubated with secondary antibody diluted in permeabilization buffer (goat anti-mouse IgG conjugated to Alexa-Fluor 488, Invitrogen, 5 µg/mL or goat anti-rabbit IgG conjugated to Alexa-Fluor 488, Invitrogen, 4 µg/mL) for one hour at room temperature protected from light. Cells were then subjected to another 5-6 washes in PBS over the course of 1 hr., followed by a DAPI stain. Slides were then mounted using Vectashield aqueous mounting medium (Vector Laboratories, CA) and stored at 4°C.

Confocal Microscopy and Image Analysis

Slides were imaged on a DeltaVision Spectris confocal fluorescent microscope (Applied Precision) using a 60x oil immersion objective. The spiral mosaic algorithm on SoftWorX was used to automate imaging of a 5x5 grid of each well.

Colocalization analysis was performed using the Coloc2 plugin in ImageJ (FIJI). All images were processed using the "subtract background" command with a rolling ball radius of 50 pixels. For analysis, a region of interest was drawn around a single cell within an image, and the Pearson Correlation Coefficient was reported as a measure of colocalization between the far-red (Cy-5 conjugated DNA) channel and the FITC (endosomal marker) channel. At least 20 individual cells across multiple individual images were analyzed for each treatment group.

Animal Studies

All animal experiments were approved by the MIT Institutional Animal Care and Use Committee and were consistent with local, state, and federal regulations as applicable. For single timepoint experiments, female C57BL/6 mice (Charles River Laboratories, 18-22g) were intravenously injected with nanoparticles via the tail vein. For luciferase imaging experiments, mice were injected intraperitoneally with 130 μL of 30 mg mL^{-1} D-luciferin (PerkinElmer, MA) in PBS 24 hours after injection. 10 minutes following luciferin injection, mice were sacrificed via CO_2 asphyxiation. Six organs were collected (pancreas, spleen, kidneys, liver, lungs, and heart) and imaged for luminescence using an IVIS imaging apparatus (PerkinElmer, MA) with the luminescence being quantified using Living Image software (PerkinElmer, MA).

For time course experiments, female SKH1E mice (Jackson Labs, 18-25g) were intravenously injected with nanoparticles via the tail vein. At various time points after the injection, mice were injected intraperitoneally with D-luciferin as described for C57BL/6 mice. 5 minutes following injection, mice were anesthetized with isoflurane (typically ~5 minutes). Anesthetized mice were placed in an IVIS imaging apparatus for whole-body imaging, and luminescence was quantified using Living Image software.

For cellular localization experiments, female B6.Cg-Gt(ROSA)26Sortm14(CAG-tdTomato)Hze/J (Ai14) mice (Jackson Laboratories, 18-22g) were intravenously injected with nanoparticles via the tail vein. These nanoparticles were formulated with Cre-encoding DNA (pPGK-Cre-bpA, Addgene #11543). The Cre-encoding plasmid was generously provided as a bacterial stab by Klaus Rajewsky, and was prepared using a QIAprep Spin Miniprep Kit (Qiagen, Germany). Ai14 mice express a transgene containing a tdTomato cassette downstream of a loxP-flanked stop codon. Thus, successful expression of Cre results in constitutive cellular expression of the tdTomato fluorophore.[56] 48 hours post-injection, mice were sacrificed via CO_2 asphyxiation and their lungs

were harvested for single cell processing. Saline-treated wild type C57BL/6 mice were used as controls for experiments probing gross immune and endothelial expression.

Flow Cytometry

For cell cycle analysis experiments HeLa cells were seeded onto a 6 well plate at a concentration of 150,000 cells/mL. 24 hours after seeding, some HeLa cells were treated with 2 mM thymidine, while others remained untreated. 24 hours after thymidine treatment, cells were removed from the plate via trypsinization. Cells were then diluted in serum-containing media to inactivate trypsin and were passed through a 40 μm filter. Next, cells were centrifuged to remove supernatant, and were subject to an additional wash/centrifugation step in PBS. Cells were then fixed and permeabilized in absolute ethanol at -20ºC overnight. Following fixation, the cell/ethanol suspension was diluted in flow buffer (PBS containing 0.5% BSA and 2 mM EDTA) and centrifuged. Following supernatant removal, cells were washed an additional time in flow buffer. Cells there then treated with RNAse A (Thermo Fisher, MA) at a concentration of 10 μg/mL and incubated for 30 minutes at 37ºC. Following RNAse treatment, cells were treated with propidium iodide (Thermo Fisher, MA) at a 1:1000 dilution v/v for 20 minutes at 4ºC. Cells were then washed 2-3x in ice cold flow buffer and analyzed for propidium iodide fluorescent intensity (using a phycoerythrin filter set) on a BD LSR II cytometer (BD Biosciences, MA). Data was analyzed using FlowJo Software (Ashland, OR).

For *in vivo* cell localization experiments, lungs were digested in a mixture of collagenase I (450 U), collagenase XI (125 U), and DNase I (2 U) in 1 mL PBS at 37ºC with constant agitation for 1 hr. The digest was passed through a 70 μm filter, followed by centrifugation. The supernatant was then removed, and cells were treated with red blood cell lysis buffer for 5 min at 4ºC. The lysis buffer was then quenched with PBS, and the cells were then centrifuged again with the supernatant removed afterwards. The cells were then suspended in flow buffer (PBS containing 0.5% BSA and 2 mM EDTA) and passed through a 40 μm filter. Cells were incubated with viability dye (eBioscience Fixable Viability Dye eFluor 780, Invitrogen) at a 1:1000 dilution at 4°C for 20 minutes, followed by a wash with flow buffer. Surface staining of cells with fluorescent antibodies was then performed in flow buffer for 30 minutes (CD31-AF488, Biolegend, MEC1.3; CD45-BV421, BioLegened, 104). Each antibody was diluted at 1:300 v/v. Following surface staining, cells were washed twice with and then re-suspended in flow buffer for analysis. Gating strategies for cell population identification can be found in Figure S6. Data was collected using a BD LSR II or Fortessa cytometer (BD Biosciences) and analyzed with FlowJo software (Ashland, OR).

Statistics

Data were expressed as mean ± SD for groups of at least three replicates. All statistical analysis were performed using an unpaired, two-tailed student's t test in Graphpad Prism 7.

Acknowledgements

The authors would like to acknowledge project funding from Translate Bio (Lexington, MA) and support from the Marble Center for Cancer Nanomedicine, and Cancer Center Support (core) Grant (P30-CA14051) from the National Cancer Institute. AKP gratefully acknowledges The Royal

Society Research Grant (RGS\R2\192353), and National Institute for Health Research Imperial Biomedical Research Centre award (RDF04). We thank the Koch Institute Swanson Biotechnology Center for technical support, specifically the Nanotechnology Materials core, Flow Cytometry core and Preclinical Imaging & Testing core.

Data Availability

The raw/processed data required to reproduce these findings can be shared by the author upon request.

References:

[1] S. T. Crooke, C. F. Bennett, *Annual Rev. Pharmacol. Toxicol.* **1996**, *19*, 107.
[2] S. T. Crooke, S. Wang, T. A. Vickers, W. Shen, X. Liang, *Nature Biotechnology* **2017**, *35*, 230.
[3] R. Kanasty, J. R. Dorkin, A. Vegas, D. Anderson, *Nature materials* **2013**, *12*, 967.
[4] S. F. Dowdy, *Nat Biotech* **2017**, *35*, 222.
[5] S. D. Patil, D. G. Rhodes, D. J. Burgess, *The AAPS Journal* **2005**, *7*, E61.
[6] D. Ibraheem, a Elaissari, H. Fessi, *International journal of pharmaceutics* **2014**, *459*, 70.
[7] J. C. Kaczmarek, P. S. Kowalski, D. G. Anderson, *Genome Medicine* **2017**, *9*, 60.
[8] K. J. Kauffman, M. J. Webber, D. G. Anderson, *Journal of Controlled Release* **2015**, DOI 10.1016/j.jconrel.2015.12.032.
[9] G. Sahay, D. Y. Alakhova, A. V Kabanov, *Journal of controlled release : official journal of the Controlled Release Society* **2010**, *145*, 182.
[10] T. P. Prakash, C. R. Allerson, P. Dande, T. A. Vickers, N. Sioufi, R. Jarres, B. F. Baker, E. E. Swayze, R. H. Griffey, B. Bhat, *Journal of Medicinal Chemistry* **2005**, *48*, 4247.
[11] K. J. Kauffman, F. F. Mir, S. Jhunjhunwala, J. C. Kaczmarek, J. E. Hurtado, J. H. Yang, M. J. Webber, P. S. Kowalski, M. W. Heartlein, F. DeRosa, D. G. Anderson, *Biomaterials* **2016**, *109*, 78.
[12] K. Karikó, H. Muramatsu, F. a Welsh, J. Ludwig, H. Kato, S. Akira, D. Weissman, *Molecular Therapy* **2008**, *16*, 1833.
[13] Y.-L. Chiu, T. M. Rana, *RNA* **2003**, *9*, 1034.
[14] K. J. Kauffman, J. R. Dorkin, J. H. Yang, M. W. Heartlein, F. DeRosa, F. F. Mir, O. S. Fenton, D. G. Anderson, *Nano Letters* **2015**, *15*, 7300.
[15] H. Yin, C.-Q. Song, S. Suresh, Q. Wu, S. Walsh, L. H. Rhym, E. Mintzer, M. F. Bolukbasi, L. J. Zhu, K. Kauffman, H. Mou, A. Oberholzer, J. Ding, S.-Y. Kwan, R. L. Bogorad, T. Zatsepin, V. Koteliansky, S. A. Wolfe, W. Xue, R. Langer, D. G. Anderson, *Nature Biotechnology* **2017**, *35*, 1179.
[16] J. D. Finn, A. R. Smith, M. C. Patel, L. Shaw, M. R. Youniss, J. van Heteren, T. Dirstine, C. Ciullo, R. Lescarbeau, J. Seitzer, R. R. Shah, A. Shah, D. Ling, J. Growe, M. Pink, E. Rohde, K. M. Wood, W. E. Salomon, W. F. Harrington, C. Dombrowski, W. R. Strapps, Y. Chang, D. V Morrissey, *Cell reports* **2018**, *22*, 2227.
[17] Y. Rui, M. Varanasi, S. Mendes, H. M. Yamagata, D. R. Wilson, J. J. Green, *Molecular Therapy - Nucleic Acids* **2020**, *20*, 661.
[18] A. Fasbender, J. Zabner, B. G. Zeiher, M. J. Welsh, *Gene Therapy* **1997**, *4*, 1173.
[19] U. Sahin, K. Karikó, Ö. Türeci, *Nature Reviews Drug Discovery* **2014**, *13*, 759.
[20] L. Zangi, K. O. Lui, A. von Gise, Q. Ma, W. Ebina, L. M. Ptaszek, D. Später, H. Xu, M. Tabebordbar, R. Gorbatov, B. Sena, M. Nahrendorf, D. M. Briscoe, R. a Li, A. J. Wagers, D. J. Rossi, W. T. Pu, K. R. Chien, *Nature biotechnology* **2013**, *31*, 898.
[21] V. Presnyak, N. Alhusaini, Y. Chen, S. Martin, N. Morris, N. Kline, S. Olson, D. Weinberg, K. E. Baker, B. R. Graveley, J. Coller, *Cell* **2015**, *160*, 1111.
[22] M. S. D. Kormann, G. Hasenpusch, M. K. Aneja, G. Nica, A. W. Flemmer, S. Herber-Jonat, M. Huppmann, L. E. Mays, M. Illenyi, A. Schams, M. Griese, I. Bittmann, R. Handgretinger, D. Hartl, J. Rosenecker, C. Rudolph, *Nature Biotechnology* **2011**, *29*, 154.
[23] F. DeRosa, B. Guild, S. Karve, L. Smith, K. Love, J. R. Dorkin, K. J. Kauffman, J. Zhang, B. Yahalom, D. G. Anderson, M. W. Heartlein, *Gene Therapy* **2016**, *23*, 699.
[24] J. Jemielity, T. Fowler, J. Zuberek, J. Stepinski, M. Lewdorowicz, A. Niedzwiecka, R. Stolarski, E. Darzynkiewicz, R. E. Rhoads, *RNA (New York, N.Y.)* **2003**, *9*, 1108.
[25] A. J. Mahiny, A. Dewerth, L. E. Mays, M. Alkhaled, B. Mothes, E. Malaeksefat, B. Loretz, J. Rottenberger, D. M. Brosch, P. Reautschnig, P. Surapolchai, F. Zeyer, A. Schams, M. Carevic, M. Bakele, M. Griese, M. Schwab, B. Nürnberg, S. Beer-Hammer, R. Handgretinger, D. Hartl, C.-M. Lehr, M. S. D. Kormann, *Nature Biotechnology* **2015**, *33*, 584.
[26] J. C. Kaczmarek, A. K. Patel, K. J. Kauffman, O. S. Fenton, M. J. Webber, M. W. Heartlein, F. DeRosa, D. G. Anderson, *Angewandte Chemie International Edition* **2016**, *55*, 13808.

[27] J. C. Kaczmarek, K. J. Kauffman, O. S. Fenton, K. Sadtler, A. K. Patel, M. W. Heartlein, F. Derosa, D. G. Anderson, *Nano Letters* **2018**, *18*, 6449.

[28] G. T. Zugates, W. Peng, A. Zumbuehl, S. Jhunjhunwala, Y.-H. Huang, R. Langer, J. A. Sawicki, D. G. Anderson, *Molecular Therapy* **2007**, *15*, 1306.

[29] J. C. Sunshine, M. I. Akanda, D. Li, K. L. Kozielski, J. J. Green, *Biomacromolecules* **2011**, *12*, 3592.

[30] S. Y. Tzeng, J. J. Green, *Advanced Healthcare Materials* **2013**, *2*, 467.

[31] A. A. Eltoukhy, D. Chen, C. A. Alabi, R. Langer, D. G. Anderson, *Advanced Materials* **2013**, *25*, 1487.

[32] A. A. Eltoukhy, D. J. Siegwart, C. A. Alabi, J. S. Rajan, R. Langer, D. G. Anderson, *Biomaterials* **2012**, *33*, 3594.

[33] C. W. Jung, P. Jacobs, *Magnetic Resonance Imaging* **1995**, *13*, 661.

[34] Z. Y. Chen, C. Y. He, A. Ehrhardt, M. A. Kay, *Molecular Therapy* **2003**, *8*, 495.

[35] L. M. Kranz, M. Diken, H. Haas, S. Kreiter, C. Loquai, K. C. Reuter, M. Meng, D. Fritz, F. Vascotto, H. Hefesha, C. Grunwitz, M. Vormehr, Y. Hüsemann, A. Selmi, A. N. Kuhn, J. Buck, E. Derhovanessian, R. Rae, S. Attig, J. Diekmann, R. A. Jabulowsky, S. Heesch, J. Hassel, P. Langguth, S. Grabbe, C. Huber, Ö. Türeci, U. Sahin, *Nature* **2016**, *534*, 396.

[36] K. a Whitehead, J. Matthews, P. H. Chang, F. Niroui, J. R. Dorkin, M. Severgnini, D. G. Anderson, *ACS nano* **2012**, *6*, 6922.

[37] J. Huotari, A. Helenius, *EMBO Journal* **2011**, *30*, 3481.

[38] G. Sahay, W. Querbes, C. Alabi, A. Eltoukhy, S. Sarkar, C. Zurenko, E. Karagiannis, K. Love, D. Chen, R. Zoncu, Y. Buganim, A. Schroeder, R. Langer, D. G. Anderson, *Nature biotechnology* **2013**, *31*, 653.

[39] S. Patel, N. Ashwanikumar, E. Robinson, A. DuRoss, C. Sun, K. E. Murphy-Benenato, C. Mihai, Ö. Almarsson, G. Sahay, *Nano Letters* **2017**, *17*, 5711.

[40] A. K. Blakney, G. Yilmaz, P. F. McKay, C. R. Becer, R. J. Shattock, *Biomacromolecules* **2018**, acs.biomac.8b00429.

[41] O. Andries, M. De Filette, J. Rejman, S. C. De Smedt, J. Demeester, M. Van Poucke, L. Peelman, C. Peleman, T. Lahoutte, N. N. Sanders, *Molecular Pharmaceutics* **2012**, *9*, 2136.

[42] Y. Wang, H. Su, Y. Yang, Y. Hu, L. Zhang, P. Blancafort, L. Huang, *Molecular Therapy* **2013**, *21*, 358.

[43] A. K. Patel, J. C. Kaczmarek, S. Bose, K. J. Kauffman, F. Mir, M. W. Heartlein, F. DeRosa, R. Langer, D. G. Anderson, *Advanced Materials* **2019**, *31*, 1805116.

[44] B. Schwanhäusser, D. Busse, N. Li, G. Dittmar, J. Schuchhardt, J. Wolf, W. Chen, M. Selbach, *Nature* **2011**, *473*, 337.

[45] V. Stonyte, E. Boye, B. Grallert, *Journal of Cell Science* **2018**, *131*, jcs220327.

[46] A. Akinc, W. Querbes, S. De, J. Qin, M. Frank-Kamenetsky, K. N. Jayaprakash, M. Jayaraman, K. G. Rajeev, W. L. Cantley, J. R. Dorkin, J. S. Butler, L. Qin, T. Racie, A. Sprague, E. Fava, A. Zeigerer, M. J. Hope, M. Zerial, D. W. Y. Sah, K. Fitzgerald, M. A. Tracy, M. Manoharan, V. Koteliansky, A. de Fougerolles, M. A. Maier, *Molecular Therapy* **2010**, *18*, 1357.

[47] J. Gilleron, W. Querbes, A. Zeigerer, A. Borodovsky, G. Marsico, U. Schubert, K. Manygoats, S. Seifert, C. Andree, M. Stöter, H. Epstein-Barash, L. Zhang, V. Koteliansky, K. Fitzgerald, E. Fava, M. Bickle, Y. Kalaidzidis, A. Akinc, M. Maier, M. Zerial, *Nature biotechnology* **2013**, *31*, 638.

[48] M. Yanez Arteta, T. Kjellman, S. Bartesaghi, S. Wallin, X. Wu, A. J. Kvist, A. Dabkowska, N. Székely, A. Radulescu, J. Bergenholtz, L. Lindfors, *Proceedings of the National Academy of Sciences* **2018**, 201720542.

[49] Z. Y. Chen, C. Y. He, L. Meuse, M. A. Kay, *Gene Therapy* **2004**, *11*, 856.

[50] D. R. Gill, S. E. Smyth, C. A. Goddard, I. A. Pringle, C. F. Higgins, W. H. Colledge, S. C. Hyde, *Gene Therapy* **2001**, *8*, 1539.

[51] Z. Y. Chen, S. R. Yant, C. Y. He, L. Meuse, S. Shen, M. A. Kay, *Molecular Therapy* **2001**, *3*, 403.

[52] N. S. Yew, M. Przybylska, R. J. Ziegler, D. Liu, S. H. Cheng, *Molecular Therapy* **2001**, *4*, 75.

[53] L. Qin, Y. Ding, D. R. Pahud, E. Chang, M. J. Imperiale, J. S. Bromberg, *Human Gene Therapy* **1997**, *8*, 2019.

[54] K. Norrman, Y. Fischer, B. Bonnamy, F. W. Sand, P. Ravassard, H. Semb, *PLoS ONE* **2010**, *5*, DOI 10.1371/journal.pone.0012413.

[55] D. Chen, K. T. Love, Y. Chen, A. A. Eltoukhy, C. Kastrup, G. Sahay, A. Jeon, Y. Dong, K. A. Whitehead, D. G. Anderson, *Journal of the American Chemical Society* **2012**, *134*, 6948.

[56] K. J. Kauffman, M. A. Oberli, J. R. Dorkin, J. E. Hurtado, J. C. Kaczmarek, S. Bhadini, J. Wyckoff, R. Langer, A. Jaklenec, D. G. Anderson, *Molecular Therapy - Nucleic Acids* **2017**, *10*, 55.